UCRL-84503
PREPRINT

APPLICATION OF A PHOTODIODE-ARRAY OPTICAL TURBULENCE SENSOR TO WIND STUDIES IN COMPLEX TERRAIN

W. M. Porch
T. J. Green

Addendum Paper for
ASCOT Program Planning Meeting
Gettysburg, PA, Apr. 15-18, 1980

April 1980

UCRL-84503

APPLICATION OF A PHOTODIODE-ARRAY OPTICAL TURBULENCE SENSOR TO WIND STUDIES IN COMPLEX TERRAIN*

W. M. Porch and T. J. Green

Addendum Paper for ASCOT Meeting
Gettysburg, Pennsylvania
April 1980

ABSTRACT

A digital photodiode-array optical turbulence sensor was used to gather data simultaneously with analog optical anemometer measurements during the July 1979 ASCOT experiment. This system provided useful information regarding the uniformity of optical turbulence used by the optical anemometer to derive cross-path wind speeds. Wind speeds derived from digital analysis of the photodiode-array intensities also provided an independent measure of the cross-path wind speed. Close agreement was found between these two measures of the wind. The optical turbulence along the 625 meter light path was found to be predictably uniform when averaged over a 10 minute time period at night during drainage wind conditions. At sunrise one side of the valley was heated first and a nonuniform optical turbulence pattern resulted.

*This work was performed under the auspices of the U. S. Department of Energy by the Lawrence Livermore National Laboratory under contract No. W-7405-Eng-48.

INTRODUCTION

The two companion papers to this addendum paper describe results using a laser space-averaging optical anemometer during the July, 1979 ASCOT experiment in the complex terrain Geyser's region.[1,2] Since this instrument depends on spacial uniformity of optical turbulence to represent a spacially averaged wind and index of refraction structure parameter C_n, it is important to understand when and over what averaging times this assumption is valid in complex terrain. To do this, a simultaneous measurement of optical turbulence along a closely parallel path was made using a digital photodiode-array incoherent light system from selected periods during the drainage wind experimental period. Lawrence and Strohbehn[3] have shown how the correlation function for irradiance fluctuations can be used to derive information regarding the uniformity of optical turbulence along a light path. This function along with an independent measurement of the cross-path wind speed was determined from the digitized signals on the photodiode-array elements. This digital technique has several advantages over analog wind systems in that many different analysis techniques can be used on the same set of data. A relative disadvantage is that since each scan represented two seconds of data digitized at 500 Hz, for 16 separate channels, 80 floppy disks are required to store 8 hours of 1 minute data. However, for short intensive experiment periods like the Geyser's study, the results showed the two systems complimented each other quite well.

The results of this comparison showed the following information regarding uniformity of optical turbulence and wind speeds during drainage and morning upslope winds across Anderson Creek:

1. During drainage conditions the irradiance correlation function showed a normal but variable decrease with cell separation associated with random inhomogeneities in optical turbulence over a two second time period.
2. Ten minute averaging of 10 two second samples removed almost all this variability.
3. However, after sunrise the receiver side of the light path was preferentially heated and the correlation function showed a sudden change (a faster dropoff with cell separation).
4. Wind speeds derived by both the analog laser and incoherent digital systems compared well (within 0.8 m/s) during the whole period even though the spacial filtering for the two systems causes each to have a somewhat different wind weighting function along the path.

The combination of the digital and analog systems allowed ten days of continuous wind and optical turbulence data from the analog system with periodic intensive documentation of the optical turbulence from the digital system.

RESULTS

The experimental set-up and results from the analog laser cross-wind anemometer has been described in the two companion papers from the Gettysburg ASCOT meeting. Figure 1 shows the experimental arrangement for the digital photodiode-array optical turbulence system. The light path was parallel to the laser system (separated by about 1.5 meters) over the same 625 meter path length. The transmitter consisted of a 15 cm mirror with a small white light source at the focus. The existing

light beam size was stopped down to a diameter of 11.5 cm. The receiving optics consisted of a 30.5 cm reflecting telescope with a transfer lens, cylindrical lens and a linear 16 element photodiode-array inside the effective focus of the telescope. The photodiode-array was aligned so that the center half of the focused light illuminated all 16 cells. This was done to limit diffraction effects and small nonlinearities in the photocell responses. The cylindrical lens was used to expand the effective vertical extent of the cells to limit partial coherence effects. The photodiode-array was clocked at 500 Hz and the analog signal from each cell was digitized for 1024 scans (about 2 seconds). These signals were then sampled by a microcomputer and stored on floppy disk media. These data were then analyzed after the experiment. Data were taken at selected periods during each of the 5 nighttime drainage intensive experiment periods. In this paper, we will only describe the results from the data taken on 19 July 1979. Alignment problems on subsequent nights made much of this later data suspect. Also, this was the period chosen for comparison of acoustic and optical turbulence in one of the companion papers.

The theory of how optical turbulence is used to derive spacially averaged cross-wind speeds have been well described by others.[4,5] The following assumptions about the statistical properties of the optical and atmospheric turbulence are necessary for the derived wind speed to be correct and represent a spacial average with a weighting function peaked at the center of the path and smoothly decaying the zero at each end:

1. The absence of optical turbulence saturation effects (this condition was met throughout the experiment).

2. Kolmogorov inertial subrange atmospheric turbulence statistics for the scales of turbulence affecting the optical measurements (i.e., scales greater than 20 millimeters and less than 15 meters).

3. Homogeneous isotropic optical turbulence along symmetric parts of the path (Gaussian log amplitude fluctuations and therefore log-normal intensity fluctuations are also assumed).

It is this third assumption which is the most difficult to justify in complex terrain even over symmetrically varying topography. Lawrence and Strohbehn[3] have shown how the irradiance correlation function can be used to demonstrate non-symmetrical optical turbulence along a light path. The principal application of the digital-photodiode array system was to monitor this function.

Figure 2 shows two examples of the irradiance correlation function on the morning of July 19. These two samples were chosen to show the effect of nonuniform heating of the rising sun on the receiver side of the optical path at 0635 PST when compared to a typical correlation function during the drainage wind night (0423 PST). The values for the cell separations shown in Figure 2 represent the effective size of the distance between cells through the telescope optical system. For a point light source and point receivers, the correlation function should reach zero before one Fresnel zone[4] ($\sim$2 cm). However, the extended light source size and detector size has the effect of extending the significant correlation sizes to larger values so that the function at 0423 PST represents the more symmetric optical turbulence distribution of the two situations shown in Figure 2. A parameter r_c is defined to be that value of cell separation at which the correlation drops to 33%. This

parameter is used to show how the irradiance correlation function varied throughout the night and morning. Figure 3 plots r_c versus time again for 19 July 1979. The dots represent individual 2 second samples and the open circles and line represent 10 minute averages. This figure shows that over a 10 minute average most of the inhomogeneity of the path averaged optical turbulence is smoothed out. Figure 3 also shows the rapid change in r_c after the sun began preferentially heating the receiver side of the optical path (about 0530 PST) and return to a more symmetric pattern after about 0730 PST. Figure 4 shows these two periods designated on plots of acoustic sounder return strength (function of C_T the temperature structure parameter) and the standard deviation of the log intensity of the laser σ_I (function of C_N the index of refraction structure parameter). This figure shows that though the rising sun disrupts the horizontal optical turbulence homogeneity it stabilizes the vertical temperature differences decreasing optical and acoustic turbulence.

The digital photodiode-array system was also used to provide an independent measure of the cross-path wind speed. By summing the left and right halves of the array independently, the correlation function can be used to interpret the wind speed. The weighting function for an extended incoherent wind speed determination from the slope of the correlation at zero time lag is more peaked than the analogous weighting function using a laser.[6] Therefore, a strong relationship between the two techniques is another indication that the weighting function is symmetric in complex terrain when a proper averaging time is chosen. Figure 5 shows a scatter plot with 10 and 30 minute averaging times between the two techniques. The rising sun generated the eastward slope

winds (shown as negative values) and there is somewhat more scatter in these results than the westward drainage wind region (positive wind speeds). The transition between drainage and upslope wind occurred at different times at the two ends of the path. This is shown in Table 1. Table 1 shows a 10 minute average time history of the parameters describing cross path wind speed and optical turbulence. It is interesting to note that the transition from downslope to upslope wind occurs simultaneously measured with the two optical anemometer systems. This transition is between the time this 180^{o} wind direction change occurred on the heated side of the path (Aminoil pipeyard) and the shadowed side (Thorn 7). The optical turbulence parameters anticipate this transition.

Our future plans include calibrating the photodiode-array system on an anemometer test range. This will allow us to include other properties of the correlation function such as the width of the peak, what frequency separation balances the functions, the time delay to maximum, the spacial filter spectral peak and the optical turbulence parameters σ_I and r_c in the wind speed and weighting function determination. This system will be used again in the September 1980 ASCOT Geyser's area experiment, and results will be compared with 7 other optical anemometer measurements.

CONCLUSIONS

The irradiance correlation function and the wind speed determined with a digital photodiode-array optical system indicates that the path averaged optical turbulence was symmetric for the particular optical path used in the July 1979 ASCOT experiment when time averages greater than 10 minutes are used. During the morning, and presumably in the evening, the optical turbulence predominates on the heated side of the light path

making the wind weighting function asymmetric. A comparison of cross-wind measurements in the morning show that the transition from downslope drainage winds to upslope winds occurred first on the heated side of the optical path, then on the two optical anemometer readings and finally 30 minutes later on the shadowed side of the path as the sun began to heat it.

ACKNOWLEDGEMENTS

The authors would like to thank D. Garka and K. Lamson who helped with the data taking, T. Galloway and J. Waidl who helped prepare the instrument and P. Gudiksen and M. Dickerson for their support.

REFERENCES

1. W. M. Porch, "Spacially-averaged and Point Measurements of Wind Variability in the Geyser's Area", Lawrence Livermore Laboratory Rept. UCRL-84092 (1980).

2. W. M. Porch, "Application of Digital Image Analysis Techniques to the Geyser's Data and Topography", ibid. UCRL-84091 (1980).

3. R. S. Lawrence and J. W. Strohbehn, "A Survey of Clear-air Propagation Effects Relevant to Optical Communications", Proceedings of the IEEE, 58 (10), pp. 1523-1545 (1970).

4. S. F. Clifford, "The Classical Theory of Wave Propagation in a Turbulent Medium", Laser Beam Propagation in the Atmosphere, ed. J. W. Strohbehn, Springer-Verlag, N.Y. (1978).

5. R. S. Lawrence, G. R. Ochs and S. F. Clifford, "Use of Scintillations to Measure Average Wind Across a Light Beam", Applied Optics 11 (2) (1972).

6. G. R. Ochs and T-I Wang, "Finite Aperture Optical Scintillometer for Profiling Wind and C_n^2", Applied Optics 17 (23) (1978).

FIGURE CAPTIONS

Fig. 1 Block diagram of photodiode-array wind and optical turbulence system.

Fig. 2 Plots of typical irradiance correlation functions for nighttime drainage (0423 PST) and after sunrise (0635 PST) versus equivalent cell separation for 2 seconds of optical turbulence data sampled at 500 Hz.

Fig. 3 Plot of the time history of the correlation distance parameter r_c (distance correlation goes below 33%) during the morning of 19 July 1979.

Fig. 4 Nighttime drainage ($r_c \approx 2.25$ cm) and heated slope inhomogeneity of optical turbulence ($r_c \approx 1.25$ cm) periods separated from plots of optical turbulence parameter σ_1 and acoustic turbulence (as a function of C_T) versus time for the morning of 19 July 1979.

Fig. 5 Scatter plot of cross-path wind speeds determined using digital photodiode-array incoherent light system versus wind speeds determined from analog laser system for 10 and 30 minute averaging times.

Table 1: Ten and Thirty Minute Averages of Wind and Optical Turbulence Parameters on the Morning of July 19 in the Geyser's Region

Time (PST)	Laser Anemometer Cross-Path Wind Speed (m/s) (10 min. avg.)	Thorn 7 Cross-Path Wind Speed Component (m/s) (10 min. avg.)	Aminoil Pipeyard Cross-Path Wind Speed Component (m/s) (30 min. avg.)	Standard Deviation of Log of Laser Light Intensity (σ_I) (10 min. avg.)	Slope of Time-lagged Correlation Function from from Photodiode-Array System (10 min. avg.)	Spacial Correlation Distance from Photodiode Array System (cm) r_c (10 min. avg.)
0420	2.8	1.27		0.11	.075	2.21
0430	2.3	0.19	0.32	0.11	.064	2.90
0440	2.1	0.22		0.12	.054	2.05
0450	1.9	0.00		0.11	.052	2.34
0500	1.7	-0.10	0.19	0.10	.053	2.40
0510	1.8	0.59		0.09	.038	2.33
0520	1.8	1.50		0.09	.053	2.44
0530	1.7	0.92	0.28	0.09	.067	2.46
0540	1.8	0.91		0.08	.029	1.74
0550	0.6	0.73		0.09	.027	1.70
0600	0.5	0.63	0.11	0.06	.008	1.19
0610	0.5	0.42		0.04	.020	1.16
0620	0.7	0.85		0.05	.029	1.14
0630	0.9	0.91	-0.35	0.03	.021	1.18
0640	-0.1	0.19		0.05	-.012	1.19
0650	-0.4	-0.05		0.04	-.013	1.09
0700	-0.7	-0.90	-0.78	0.05	-.014	0.99
0710	-0.8	-0.66		0.05	-.013	1.27
0720	-0.8	-0.57		0.08	-.022	1.18
0730	-0.9	-0.43	-0.76	0.09	-.031	1.15
0740	-0.7	-0.06		0.10	-.026	3.42
0750	-0.7	-0.18		0.10	-.015	3.47

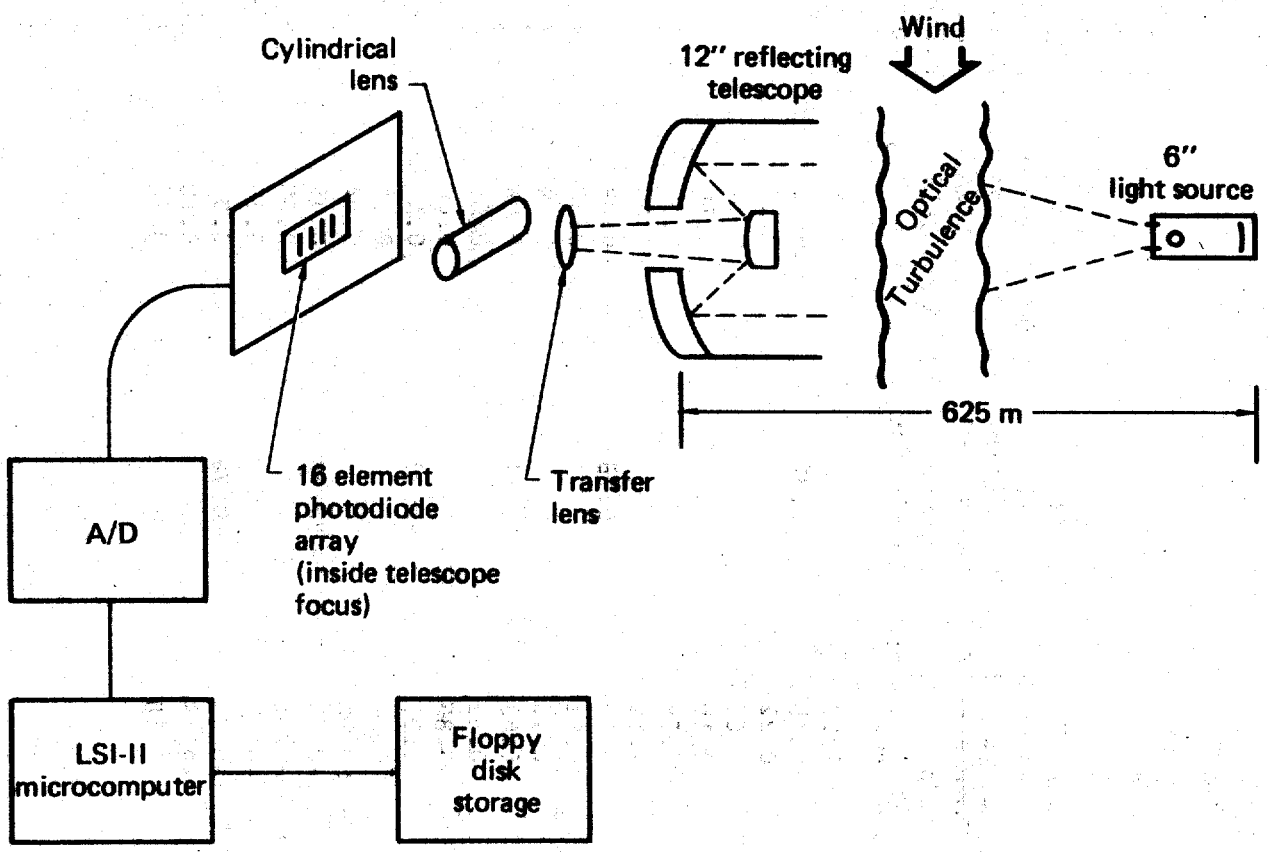
Cylindrical lens
12" reflecting telescope
Wind
Optical Turbulence
6" light source
625 m
16 element photodiode array (inside telescope focus)
Transfer lens
A/D
LSI-11 microcomputer
Floppy disk storage

Figure 1.

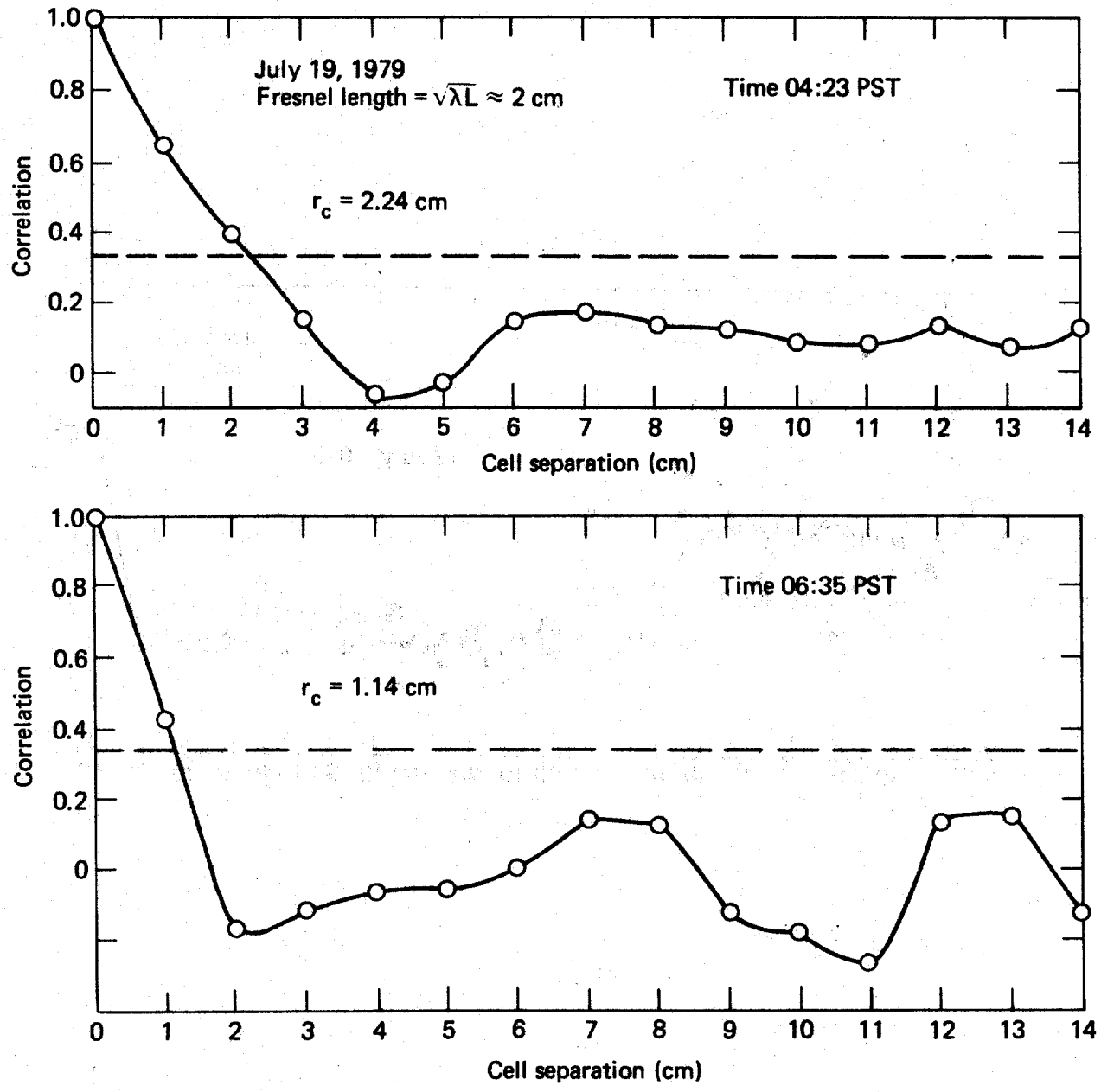
July 19, 1979
Fresnel length = $\sqrt{\lambda L} \approx 2$ cm
Time 04:23 PST
r_c = 2.24 cm
Correlation
Cell separation (cm)
Time 06:35 PST
r_c = 1.14 cm
Correlation
Cell separation (cm)

Figure 2.

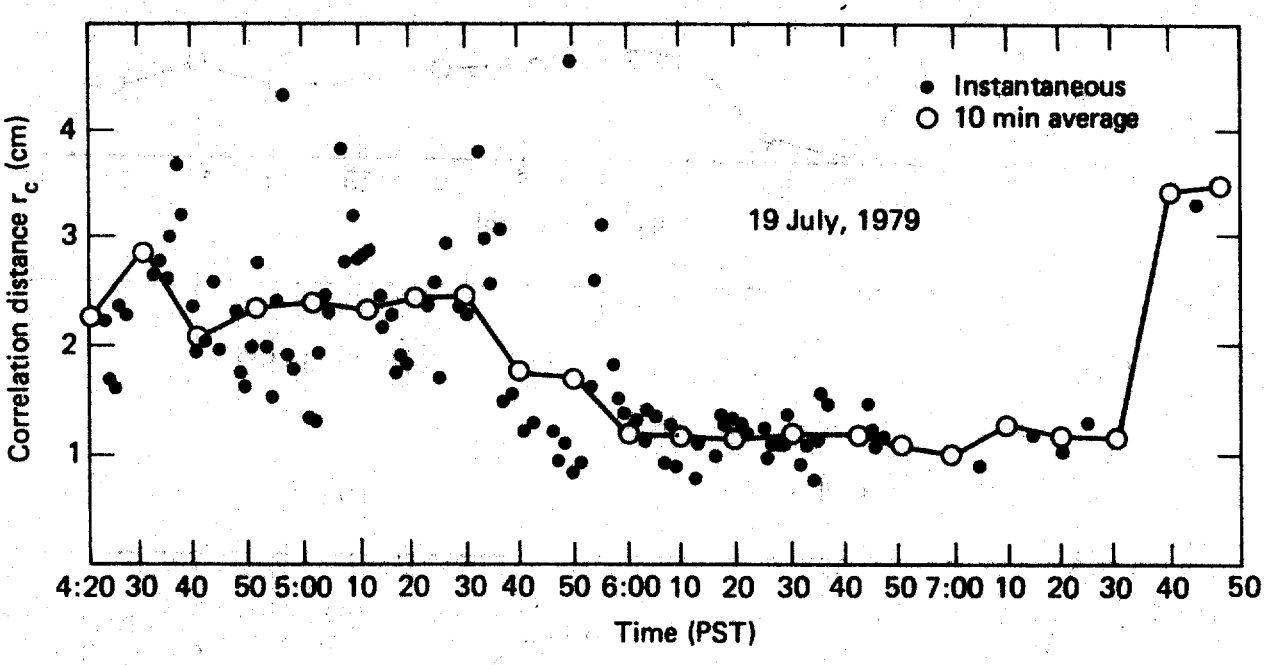
Instantaneous
10 min average
19 July, 1979
Correlation distance r_c (cm)
1
2
3
4
4:20 30 40 50 5:00 10 20 30 40 50 6:00 10 20 30 40 50 7:00 10 20 30 40 50
Time (PST)

Figure 3.

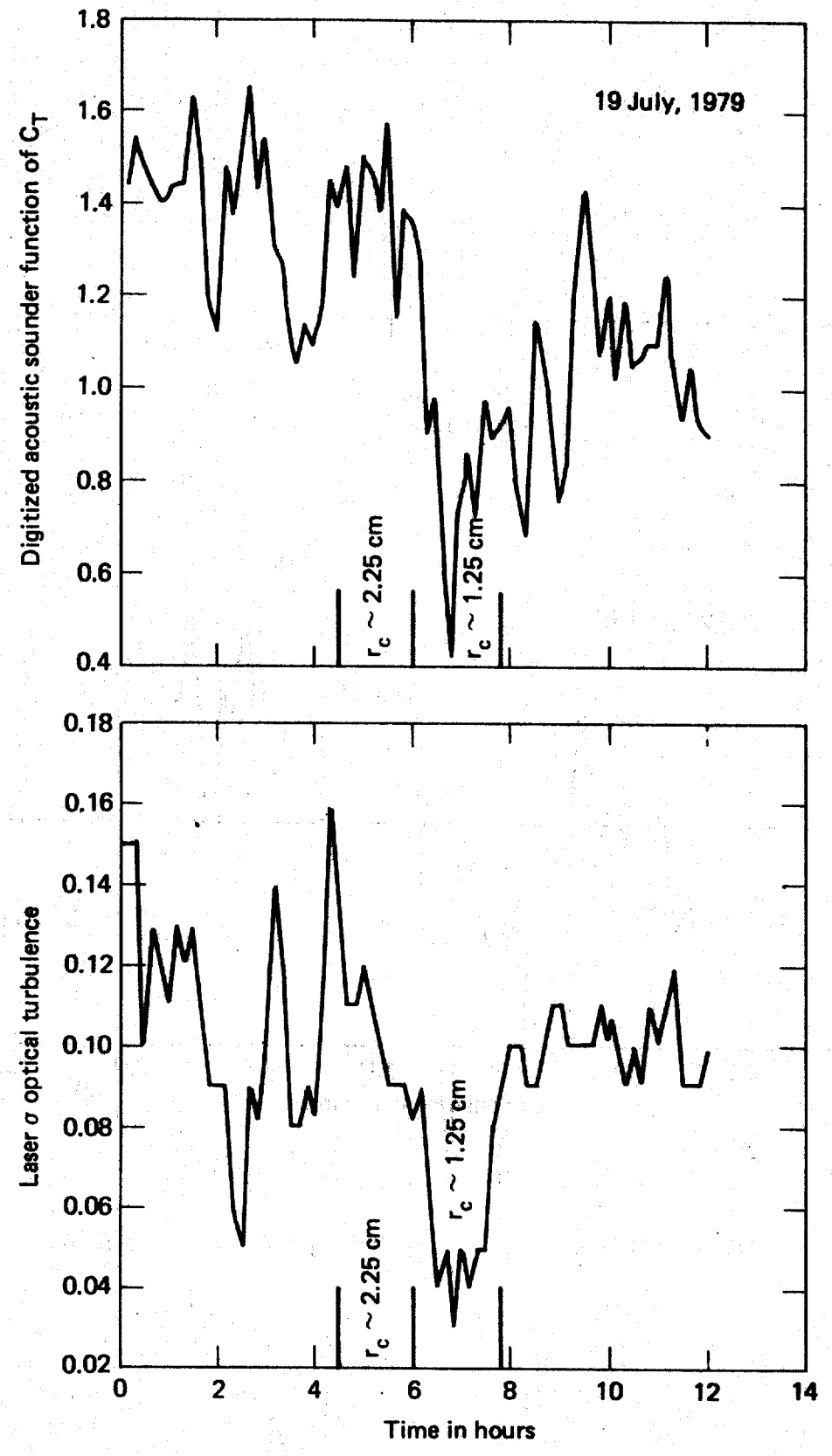
19 July, 1979
Digitized acoustic sounder function of C_T
Laser σ optical turbulence
$r_c \sim 2.25$ cm
$r_c \sim 1.25$ cm
$r_c \sim 2.25$ cm
$r_c \sim 1.25$ cm
Time in hours
1.8
1.6
1.4
1.2
1.0
0.8
0.6
0.4
0.18
0.16
0.14
0.12
0.10
0.08
0.06
0.04
0.02
0
2
4
6
8
10
12
14

Figure 4.

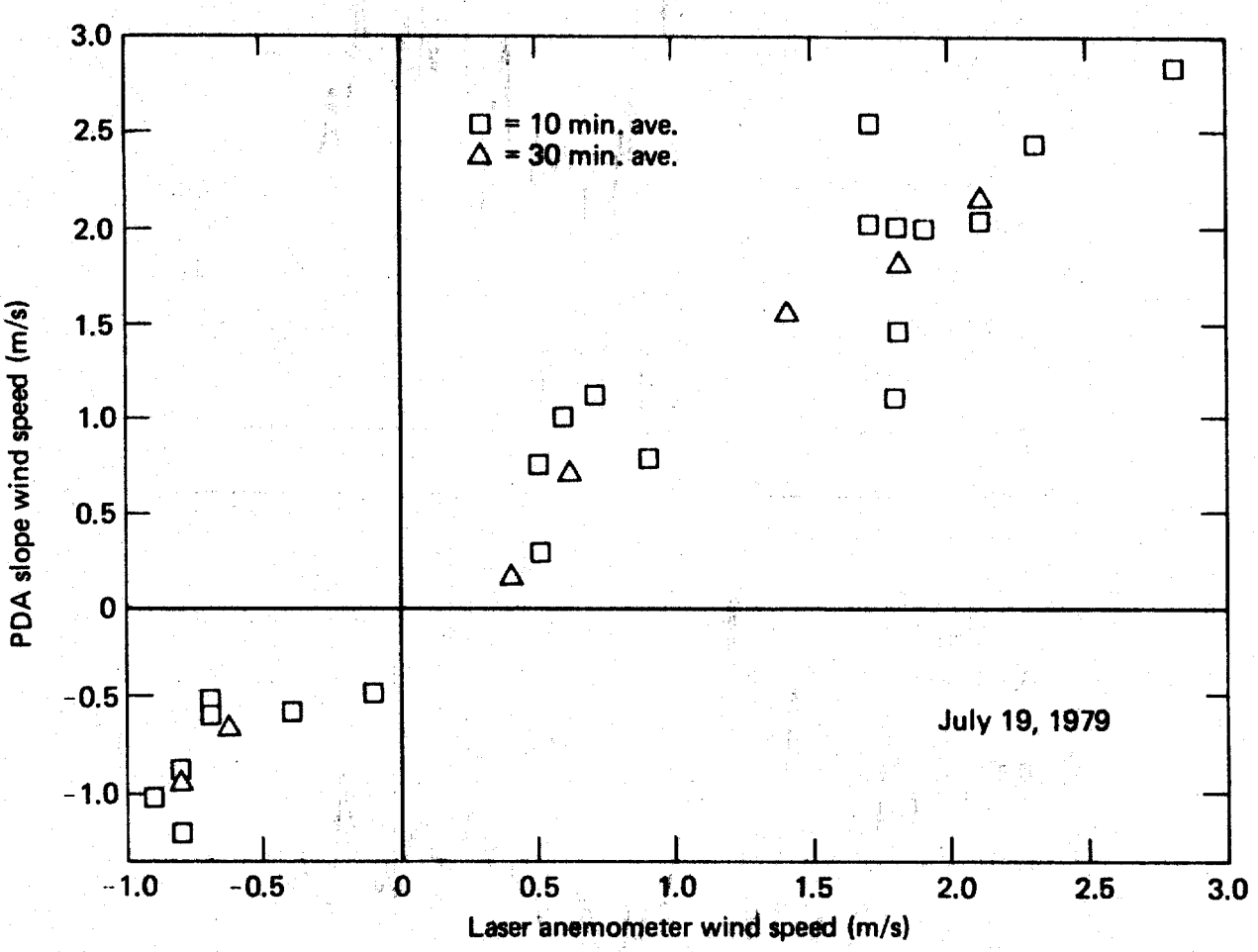
□ = 10 min. ave.
△ = 30 min. ave.
July 19, 1979
PDA slope wind speed (m/s)
Laser anemometer wind speed (m/s)
3.0
2.5
2.0
1.5
1.0
0.5
0
-0.5
-1.0
-1.0
-0.5
0
0.5
1.0
1.5
2.0
2.5
3.0

Figure 5.

Internal Distribution

L-262
M. Dickerson
H. Ellsaesser
T. R. Galloway, L-365
T. Green
P. Gudiksen
J. Knox
R. Lange
R. Lee
M. MacCracken
C. Molenkamp
R. C. Orphan
K. Peterson
D. Tuerpe
TID(15)
TIC (2)
W. Porch (30)

L-452
L. Lamson
D. Garka
J. Shinn
G. Bingham
L. Corell (10)

WMP:1229z